Inelastic Behaviors of End-plate Connections during Earthquakes and Improvement on their Rotation Capacity

Kenichi OHI, Seung-Jae LEE, Yosuke SHIMAWAKI, Hideo OHTSUKA, Ruben GUZMAN

1. Introduction

Welded connections are widely used in beam-to-column connection of steel frames as rigid connections. But some diaphragms should be welded to the joints to obtain sufficient rigidity and strength, and it is observed in the Hanshin-Awaji earthquake and the Northridge earthquake, that the strain concentration in the vicinity of the weld may cause the fracture when loaded by severe earthquakes. Instead of such a welded rigid connection, another details semi-rigidly connected by cleats and mechanical fasteners are sometimes used in European and American countries. In Japan, however, these types of semi-rigid connections are not so popular except systematically prefabricated low-rise residential buildings, usually combined with braces or skin panels. One of the reasons is that the structural design of middle-rise unbraced frame is mainly controlled by drift limitation in Japan, and the usage of semi-rigid joints will make it more stringent. Even with this disadvantage, there are various combinations of connection stiffness and strength available corresponding to various types of semi-rigid details, and then it is possible to control collapse mode and even the energy absorption capacity of frames by an appropriate choice of semi-rigid connections. In addition, stiffness and strength required for serviceability can be enhanced by adding earthquake resisting elements like braces or dampers.

In this study, two types of semi-rigidly jointed beam specimens using end-plate are fabricated and tested: One is connected by extended end-plate and the other is flush end-plate. Quasi-static cyclic loading tests are performed to identify the restoring characteristics including pinching effect, and pseudo-dynamic tests on 3-story steel frames are carried out to examine their dynamic inelastic behaviors. Furthermore, quasi-static cyclic loading tests are done to improve rotation capacity of connection considering deformation capacity of high strength bolts.

2. Brief Description of Quasi-static and Pseudo-dynamic Tests

Test setting is shown in Figure 1. Specimen consists of a beam (H-250x125x6x9, JIS SS400 Grade steel) and end-plate which is welded to the beam tip. Two types of end-plate were fabricated: one type of an end-plate was extended from both beam flanges, and the other was a flush type. They are connected to base block using torshear type high strength bolts (M16-S10T), where base block represents a rigid column-flange and its deformation is ignored here-in. For extended type, 8-bolt layout and 4-bolt layout were prepared. Specimen details are shown in Figure 2. Red-rust is given to the surface of end-plate to be contact to the column surface. Bolt-hole diameter is prepared with 2mm clearance. Specimen material test results are summarized on Table 1. Figure 3 shows measurement setup: in case of extended type with 8 bolts, in order to measure displacements 9 transducers were placed and 20 strain gauges were attached. Main displacement measure points were at beam top, end-plate uplifting, and sliding. Strain gauges were attached in beam, end-plate and high strength bolt body.

Specimen of the same configuration was commonly used for cyclic loading and pseudo-dynamic earthquake response tests. Details for the cyclic loading tests and earthquake response tests are shown in Table 2, 3 cases each and 6 cases in total. Figure 4 shows a three-story frame for the pseudo-dynamic earthquake response test. The model consists of a rigid column supported by a non-linear spring and three steel beams with end-plate

---

(1)Associate Professor, Institute of Industrial Science, University of Tokyo
(2)Research Associate, dittos. (3) Technical Associate, dittos. (4) Graduate Student, dittos.

connections. For the earthquake response test, the specimen loaded is a cantilever with end-plate attached and the remaining is simulated in the computer. Setup of the earthquake response test is the same as shown in Figure 1. A non-linear spring is inserted at column foot that follows an ideal progressive slip hysteresis model as shown in Figure 4. (Stiffness and yield strength are taken the same levels with those of the specimen of flush end-plate connection). Table 3 shows parameters of earthquake response test. Because rigid column is assumed here-in, the equation of motion can be reduced to a single-degree-of-freedom equation as follows:

$$14H^2 m\ddot{\theta} + 3M_j + M_b = -6Hm\ddot{y}_g \tag{1}$$

where m is the fictitious mass in each floor, M_j is measured restoring moment at beam-to-column connection from the loading test, M_b is the fictitious restoring moment at column-base. $\ddot{\theta}$ is the angular acceleration response, $\ddot{y}_g$ is the input ground acceleration, H is the story height. It is used El Centro NS 1940 earthquake ground motion record, the duration and the PGA of which are taken 10 second and 300 cm/sec^2, respectively.

Table 1 Mechanical Property of Materials

	σ_y (N/mm^2)	σ_u (N/mm^2)	σ_y/σ_u (%)	Elongation (%)
Beam-flange	320	465	72	27
Beam-web	345	465	73	29
End-plate	430	570	75	18

M16-S10T	
T_y(kN)	140
T_u(kN)	170

Table 2 Test Code

Type of End-plates	Number of HTB's	Loading	Test Code
Extended	8	Cyclic	E8SC
		Earthquake	E8ON
	4	Cyclic	E4SC
		Earthquake	E4ON
Flush	4	Cyclic	F4SC
		Earthquake	F4ON

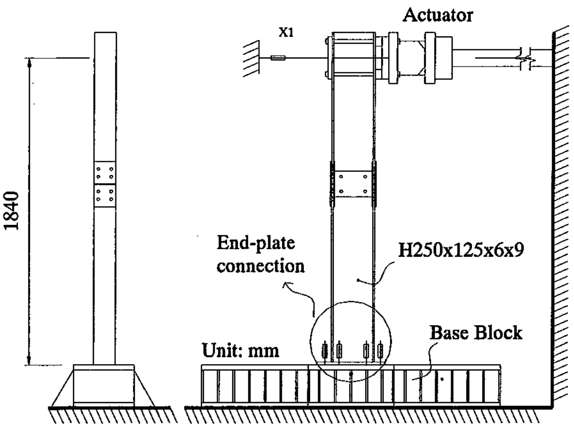

Figure 1 Test Setup

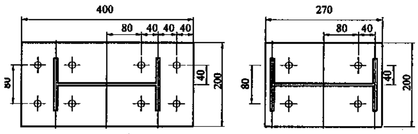

Plate thickness : 16mm

Figure 2 Details of End-plate

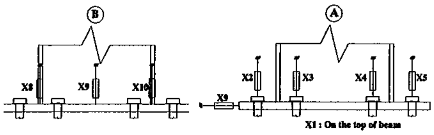

Figure 3 Measurement (E8SC)

Table 3 Parameters adopted in Earthquake Response Tests

Test Code	Natural period (Second)	Mass (kg)	M_{by} (kN*m) K_b (kN*m/rad)	Δt (sec)	Input Ground Acceleration
E8ON	0.55	5880	65.4 8450	0.005	El Centro NS 1940 300cm/sec^2 10 sec
E4ON	0.57				
F4ON	0.57				

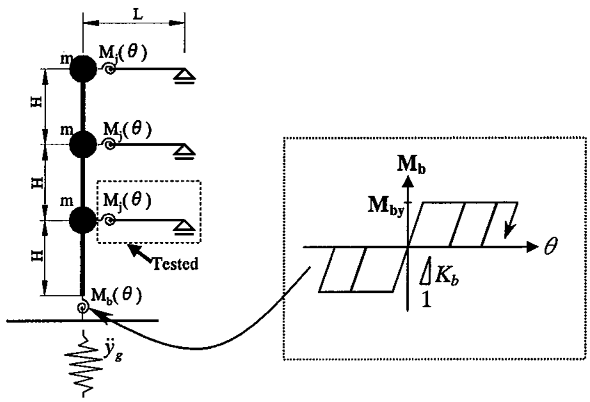

Figure 4 A Frame Model for Earthquake Response Tests

3. Cyclic Loading Test Results

Figure 5 shows the results of cyclic loading tests. Restoring moment measured is expressed non-dimensionally, referred to the full-plastic moment. The abscissa axis shows deformation angle, including beam deformation. Cyclic loading program consists of one cycle for 1/200 amplitude in deformation angle, two cycles for 1/100, one cycle for 1/50, and then monotonic loading. Deformation speed in loading is kept constant during these tests. As for the result of 8-bolt extended type, the connection showed enough strength and the hysteresis observed is caused by plastification of beam member. In case of 4-bolt extended type, at 0.035 radian (about 1/30 radian) high strength bolts were broken by tension and the test was terminated. The hysteresis in this case included some pinching. In case of flush type with 4-bolt, at 0.025 radian (1/40 radian) high strength bolts were broken and the test was terminated. The hysteresis loop is very close to an ideal progressive slip hysteresis model. Beam and end-plate remained within elastic range, also there was no sliding of end-plate. In this case, collapse mode was given by bolt failure, and then rotation capacity is governed by bolt deformation capacity. The maximum moment (M_u), yield moment (M_y), rotation capacity (θ_{jmax}), and initial stiffness (K_j) are shown in Table 4. These values are also predicted by simple analysis, and calculated ones match well with test results. As for the moment resistance calculation, the limit analysis is performed on a beam model of end-plate, where no plastic hinge is formed beneath the nuts.

Table 4 Cyclic Loading Test Results Compared with Calculated Values

Test Code	M_u(kN*m)		M_y(kN*m)		θ_{jmax}(rad)		K_j(kN*m /rad)	
	Test	Cal.	Test	Cal.	Test	Cal.	Test	Cal.
E8SC	133	113	—	113	—	—	51,000	85,000*
E4SC	83	83	54	66	0.0300	0.0304	22,000	58,000**
F4SC	71	78	50	65	0.0220	0.0197	22,000	25,000**

Plastic hinge moment and bolt resistance in the limit analysis are based on tensile strength levels to calculate ultimate moment denoted by M_u (σ_u and T_u), while yield point levels (σ_y and T_y), are used to calculate yield moment denoted by M_y. Test yield moment values are read at 1/500 in joint rotation excluding beam deformation. Rotation capacity, denoted by θ_{jmax}, at bolt breaking (also excluding beam deformation) is calculated from the collapse mode detected in the limit analysis and the bolt elongation capacity. Test values of stiffness are secant stiffness at 1/500 in joint rotation. Asterisked stiffness value is calculated from the formula of column base rigidity proposed in AIJ LSD specification. Doubly asterisked stiffness values are calculated in the same manner with the AIJ LSD formula, that is, a half time the stiffness calculated for a hinged mechanism supported by elastic bolt springs, where the mechanism is given by inserting ordinary hinges at plastic hinge location in the detected collapse mode.

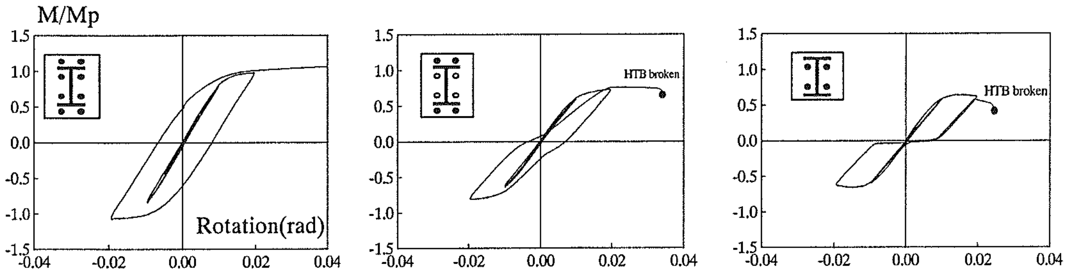

Figure 5 Cyclic Loading Test Results (E8SC, E4SC, F4SC)

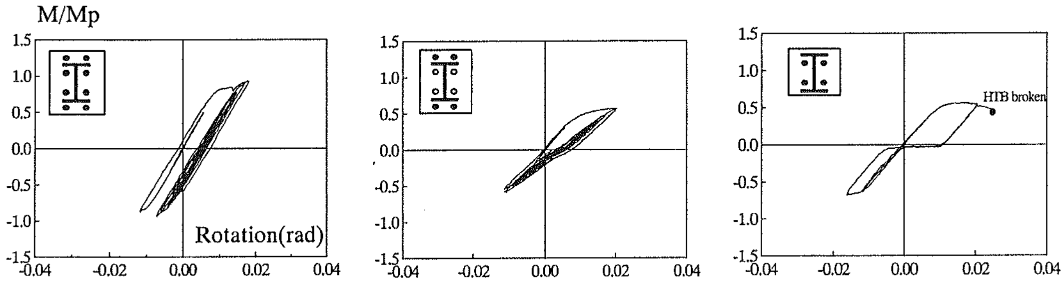

Figure 6 Earthquake Response Test Results (E8ON, E4ON, F4ON)

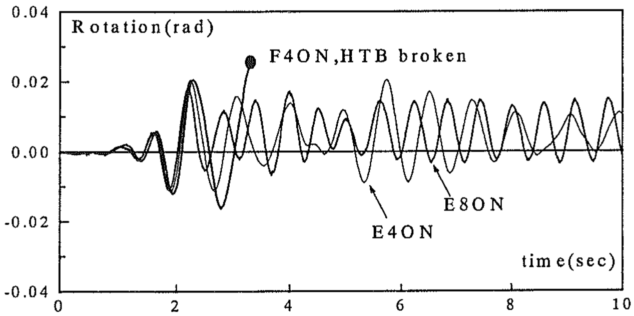

Figure 7 Time Histories of Deformation Angle

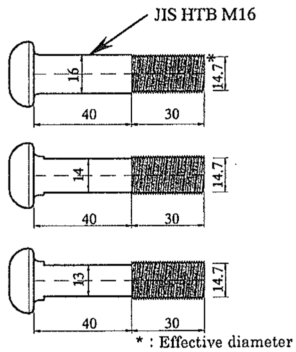

Figure 8 Shapes and Dimensions of High-deformability Bolts and JIS High-strength Bolt

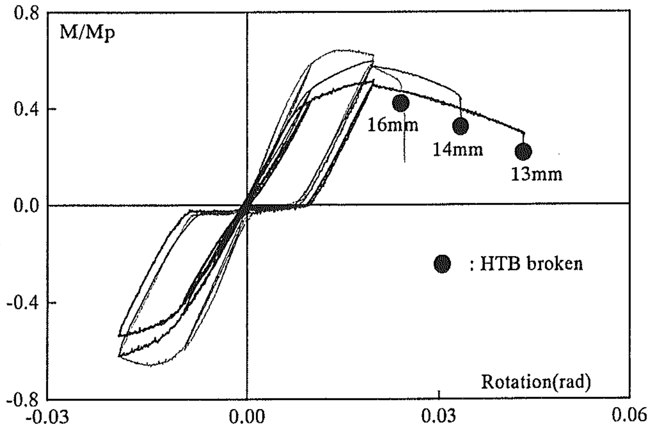

Figure 9 Cyclic Loading Test Result of High Ductility Tension Bolt

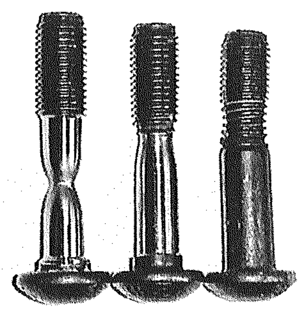

Photo 1 High Ductility Tension Bolt Failure Place

4. Online Earthquake Response Test

Figures 6 and 7 show the results of earthquake response tests on three kinds of details under the same earthquake input. As for the extended 8-bolt layout, plastification occurred in the beam member while the end-plate and the high strength bolt remained elastic. Peak angle response is 0.017 radian around at 2 seconds in time. As for the extended 4-bolt layout, slight pinching is observed in the hysteresis loop, but peak angle response remained almost the same level with the 8-bolt layout. As for the flush type, significant pinching is observed in the hysteresis loop, and then the angle response went further. Two high-strength bolts in tension side were broken at about 1/40 radian in angle response.

5. Improvement of Ductility for Flush End-plate with High Ductility High Tension Bolt

The flush type details show poor rotation capacity due to bolt breaking. To improve this capacity, a special shape of high-strength bolt is used instead of standard high-strength bolt specified in JIS. Generally with a standard bolt shape, breaking occurs at the threaded portion just beneath the nut, and the body portion remains elastic. The diameter of body portion, 16mm diameter, is reduced mechanically to 14mm and 13mm. These two kinds of special bolt, high-deformability bolts, are used in the flush type details and tested under cyclic loading. The results are shown in Figure 9. The ultimate moments are slightly reduced in the special bolt cases, but rotation capacity is much improved. The rotation capacity in the case of 13mm diameter is improved as much as almost twice of the standard case.

6. Concluding Remarks

Inelastic behaviors of three kinds of end-plate connection, extended 8-bolt layout, extended 4-bolt layout, and flush type, are examined by cyclic loading tests as well as earthquake response tests.

(1) Ultimate and yield moment resistances are well predicted by the limit analysis on a beam model of end-plate connections.
(2) Rotation capacity can be also predicted from the collapse mechanism detected and the bolt elongation capacity.
(3) Secant stiffness around yield moment has a slight discrepancy with the prediction based on the existing formula (AIJ-LSD) proposed for calculating column-base rigidity.
(4) Extended 8-bolt layout behaved as a full-strength connection, while extended 4-bolt layout behaved as a partial-strength connection with a slight pinching effect in hysteresis loop. In the earthquake response tests, however, this made no fatal difference in the peak angle response.
(5) The rotation capacity of flush type was about 1/40 radian, and this seems not always sufficient for the ultimate safety. This rotation capacity can be improved twice by use of the special bolt that has an intentionally reduced diameter in their body portion.

Reference

(1) Architectural Institute of Japan: Recommendation of Limit State Design for Steel Structures, 1998

(2) K.Ohi, H.Tanaka, K.Takanashi,: "Ultimate Strength of Steel Column Bases," Journal of Structural and Constructional Engineering, Transaction of AIJ, No.308, 1981.